LAUTECH JOURNAL OF ENGINEERING AND TECHNOLOGY 3(1): 2005. 23 – 29

FINITE ELEMENT THERMAL MODELING APPLIED TO FURNACE COOLING AND REFRACTORY DESIGN

T. K Ajiboye

Mechanical Engineering Department, Faculty of Engineering & Technology, University of Ilorin, Ilorin, Nigeria.

ABSTRACT

The application of finite element modeling to the analysis and design of furnace refractory linings provides a powerful tool for evaluating the advantages of various linings. A common approach in the finite element analysis of refractory linings is to assume perfect contact between the material/joint interfaces. The results of such analysis are extremely useful in determining the relative effectiveness of a given lining without amplifying the required amount of computer resources. Recognizing the dependence of refractory lining life on effective refractory cooling, a refractory cooling model must be able to address the region of refraction/cooling member contact more precisely. In particular, the amount of true contact area between the refractory and the cooling member must be accounted for in the form, of a thermal contact resistance. The practicality of this method requires an evaluation of the effect on refractory cooling due to the increase in true c ontact area between t he materials which c an only b e achieved i f t he m aterials h ave a v ery smooth surface area. Finite element modeling can assist in this evaluation by incorporating the effects of surface finish in the form of a thermal resistance at the material interfaces.

Nomenclature

c_p	specific heat (J/kg/K)
c	Courant number
d	thickness (m)
h	enthalpy (J/kg)
H	heat transfer coefficient term (W/m/K)
k	thermal conductivity (W/m/K)
l	length (m)
$\dot{m}$	mass flow rate (kg/s)
$\dot{M}$	gas addition rates (kg/m/s)
P	perimeter (m)
q	convective heat transfer flux (W/m2)
Q	heat absorbed per unit length (W/m)
S	diffusion number
t	time (s)
T	temperature (K)
u, v	velocity (m/s)
w	width (m)
x	furnace co-ordinate
y	inside wall co0ordinate
Greek letters	
α	strip Q_{gs} coefficient (W/m/K^4)
β	gas Q_{gs} coefficient (W/m/K^4)
γ	wall Q_{ps} coefficient (W/m/K^4)
κ	wall thermal diffusivity (m^2/s)
μ	strip Q_{gw} coefficient (W/m/K^4)
ν	gas Q_{gw} coefficient (W/m/K^4)
ε	wall Q_{gw} coefficient (W/m/K^4)
ρ	density (kg/m^3)
Subscripts	
ad	at adiabatic flame temperature
g	gas
gs	from gas to strip
gw	from gas to wall
s	strip
w	wall

INTRODUCTION

Furnace operation can be characterized by a number of characteristics, among which the most important are t emperature a nd thermal c onditions, coefficient of heat utilization and productivity [1].

The thermal performance of a furnace depends on a number of factors such as the furnace refractory lining, the temperature of fuel and the heat transfer characteristics of the furnace combustion walls and the combustion gases. The furnace temperature depends on the purpose of the furnace which determines the allowable temperature of the metal heating. Thermal conditions are essentially the time variations of thermal load which are closely related to the temperature of a furnace. In periodic furnaces which operate at a time variable temperature, the thermal load varies in time, whereas continuous furnaces operate at a constant thermal load [1].

Generally, refractories are classified by their properties and characteristics. The classification includes;

(a) By refractoriness such as common, high or highest refractories with temperatures of 1580 -1770 °C, 1770 - 2000 °C and above 2000 °C
(b) By their chemical and mineral composition such as;
   (i) Siliceous, in which the refractory base is SiO_2 (Silica, Quartzite)
   (ii) Alumina-Siliceous, where the refractory components are Al_2O_3 and SiO_2 (fireclay, semi-acid and high alumina refractoties)
   (iii) Magnesian, basaed on MgO oxide (magnesite, dolomite, forsterite, talc and spinelides)

(iv) Chromic, with the refractory base composed of Cr_2O_3 and MgO oxides (chromite, chrome-magnesite and magnesite –chromite)

(v) Carbon refractory based on carbon which include carbon and graphite refractories)

(vi) Zirconia refractories, based on ZrO_2 oxide (zirconia and zircon refractories)

(c) By the type of refractory oxide, they are divided into

(i) Acid (SiO)

(ii) Inert or natural (Al_2O_3); and

(iii) Base (MgO, CaO)

(d) By the method of manufacturing, all refractories are either natural or artificial.

In the design of a furnace, the principal materials, which play a major role in heat transfer either during heating or cooling are different types of refractories as mentioned above. These refractory linings guide in the modeling of the heat transfer process within the furnace. The only limitation imposed on these analysis include the inability to quantify furnace lining life due to the complex nature of the refractory wear beyond the scope of many analytical techniques [1,2]. However, a great deal of information can be extracted from a qualitative analysis where model parameters can be varied to determine the effect on refractory cooling.

MODEL EQUATION

The set of equations describing the furnace operation are given below. Equation (1) and (2) use a control volume method on the strip and gas, whereas equation (3) is the simple one-dimensional Fourier heat conduction equation for the wall.

$$\frac{\partial T_s}{\partial t} - V_s \frac{\partial T_s}{\partial x} = \frac{Q_{gs}}{\rho_s w_s d_s C_{ps}} \qquad \text{.............. 1}$$

$$\frac{\partial T_s}{\partial t} + V_g \frac{\partial T_g}{\partial x} = \frac{\dot{M}(h_{ad} - h_g) - Q_{gs} - Q_{gw}}{\rho_g w_g d_g C_{pg}} \qquad \text{... 2}$$

$$K_w \frac{\partial^2 T_w}{\partial y^2} = \frac{\partial T_w}{\partial t} \qquad \text{.................. 3}$$

where;

$$Q_{gs} = \alpha T_s^4 + \beta T_g^4 + \gamma T_w^4 - H_s(T_g - T_s)$$

$$Q_{gw} = \mu T_s^4 + \upsilon T_g^4 + \varepsilon T_w^4 + H_w(T_g - T_w)$$

Equation (1) describe the variation of the strip temperature with time, equation (2) the gas temperature and equation (3) the wall temperature [3]. The heat transfer by radiation in the furnace is confined to the plane normal to the direction of the strip motion. The Greek letter coefficients in the flux terms Q_{gs} and Q_{gw} include values of the Stefan Boltzmann constants, radiation shape factors and emmisivity. The H coefficients represent the convection heat transfer coefficients and include the Reynolds and Prandlt numbers.

In the furnace, when evaluating the temperatures of the strip, gas and the wall at discrete furnace points, two second- order methods are used, namely the second-order upwind and the Lax-Wendroff methods [3, 4].

The second –order upwind methods is given as;

$$T^{n+1} = -\frac{1}{2} c(1-c) T_{i-2}^n + c(2-c) T_{i+1}^4 + \frac{1}{2}(1-c)(2-c) T_i^n \qquad \text{......... .4}$$

while the Lax-Wendroff method is also given as;

$$T_i^{n+1} = \frac{1}{2} c(1+c) T_{i-1}^n - (1-c^2) T_i^n - \frac{1}{2} c(1-c) T_{1+1}^n \qquad \text{......... 5}$$

with the Courant number, $c = u \Delta t / \Delta x$.

The second-order upwind method is used on the zonal boundaries and the Lax-Wendroff method is used within each zone. The grid spacing is chosen to vary between zones, because the the zone are of different lengths as can be seen in figs. 1 and 2. During the modeling, it was observed that using a constant grid spacing throughout the whole furnace will lead to large discrepancies around the zonal boundaries, hence an optimal grid spacing for the furnace is one in which the grid spacings vary by as little as possible from one zone to the next.

As a result of the differences in the directions of motion, the form of the finite-difference methods are [5];

For the strip, the second-order upwind method given as;

$$T_{si}^{n+1} = -\frac{1}{2} c_s(1-c_s) T_{si+2}^n + c_s(2-c_s) T_{si+1}^n + \frac{1}{2}(1-c_s)(2-c_s) T_{si}^n \qquad \text{.............. 6}$$

for the gas, its second-order upwind method is;

$$T_{gi}^{n+1} = -\frac{1}{2} c_g(1-c_g) T_{gi-2}^n + c_g(2-c_g) T_{gi-1}^n + \frac{1}{2}(1-c_g)(2-c_g) T_{gi}^n \qquad \text{................ 7}$$

The second-order upwind method with the Lax-Wendroff method is given as;

$$T_{si}^{n+1} = -\frac{1}{2}c_s(1-c_s)T^n_{s\,i-1} + (1-c_s^2)T^n_{s\,i} + \frac{1}{2}c_s(1+c_s)T^n_{s\,i+1} \quad \ldots\ldots\ldots\ldots\ldots 8$$

for the strip, and

$$T_{gi}^{n+1} = \frac{1}{2}c_g(1-c_g)T^n_{g\,i-1} + (1-c_g^2)T^n_{g\,i} - \frac{1}{2}c_g(1-c_g)T^n_{g\,i+1} \quad \ldots\ldots\ldots\ldots\ldots 9$$

for the gas. The Courant number are $c_s = |v_s|\Delta t/\Delta x$ and $c_g = |v_g|\Delta t/\Delta x$.

For the wall (irrespective of the materials and thickness), a finite-difference method for the one-dimensional diffusion equation is used [6]. The steady state model for the furnace assumed that the wall was adiabatic.

FINITE ELEMENT MODELING TECHNIQUES

The finite element model was used to investigate the effects of thermal contact resistance. The main parameters in a finite element thermal model are model geometry, material properties and boundary conditions. These vary according to type of cooling arrangement (e.g.: staves vs. plate cooling), design of refractory lining, assumed furnace operating conditions and adiabatic boundaries. The following describes the development of the model for both stave and plate.

Stave Model Geometry

The approach used in predicting stave refractory cooling performance with finite element modeling initially requires the selection of the region to be analyzed. The stave lining consists of alumina refractory with silicon carbide, which is symmetrical in shape. The symmetrical nature of the stave cooling pipes allows the model to be defined at the boundary. The focus of the model was to analyze the silicon carbide brick shelf both with and without contact resistance. The thermal model consists of the silicon carbide brick, stave ledge, local stave pipes, and 50% alumina in that region. The model side boundaries are the refractory surface interface and the stave cold face. The upper and lower boundaries of the model are nearly adiabatic and were selected as such since thermal activity outside those regions will not significantly affect the calculated temperature distribution. The selected region was then divided into finite elements to establish the model geometry appropriately.

Cooling Plate Model Geometry

The first step in constructing a plate-cooling model, as for the stave, is to establish the geometric boundaries for the model such that adiabatic surfaces can be identified, thus simplifying the calculation procedure. The typical plate arrangement is shown in figure 1 below. The model boundary lines correspond to the smallest repeatable pattern in the plate arrangement indicating symmetry and thus adiabatic surfaces. When the model boundary lines have been established, a thee-dimensional representation of the refractory lining can be constructed as shown in figure 2, in which the region is divided into finite elements to establish the model geometry. The area of interest for the discussion of contact resistance is the interface between the lower portion of the upper cooling plate and the adjacent refractory [7].

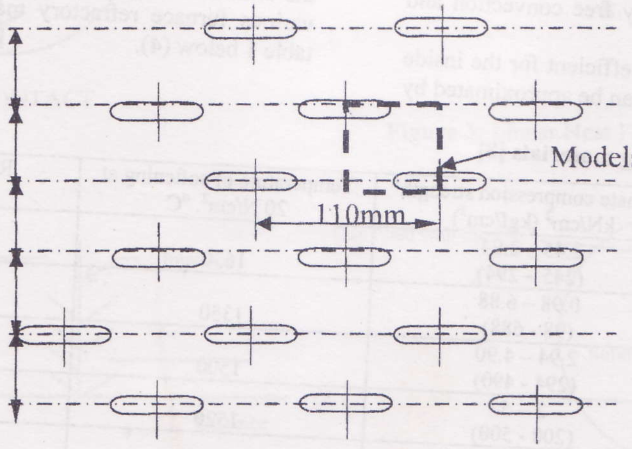

Figure 1: Typical plate Cooling Arrangement showing Model Boundary Lines

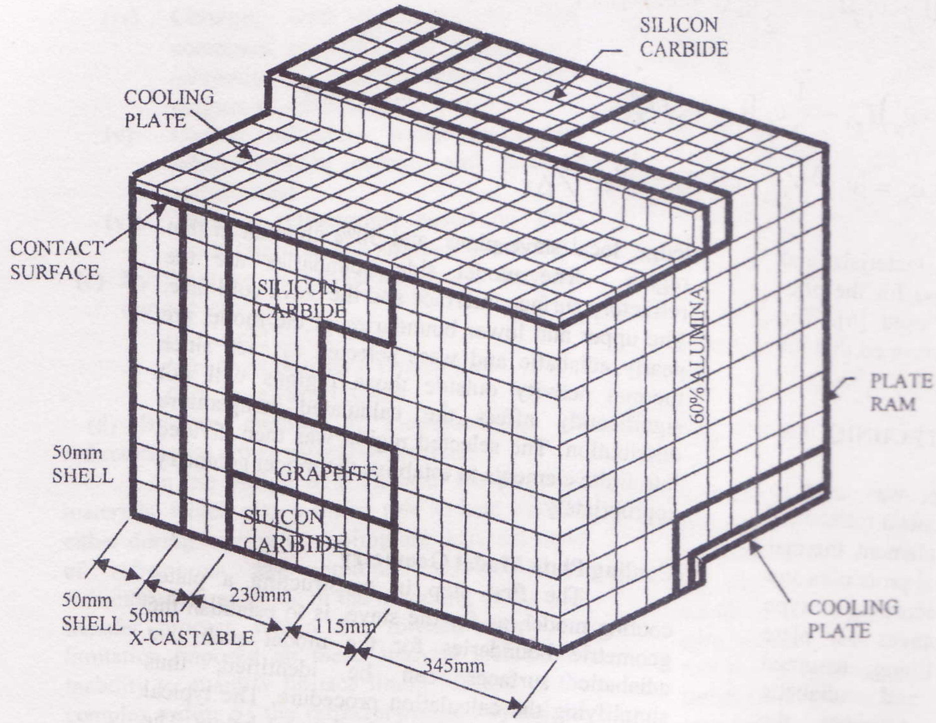

Figure 2: Typical Lining Configuration showing nodal points for particular Lining materials

Model Boundary Conditions.

After the model geometry has been established, the next step in defining the thermal model is to approximate actual furnace conditions by the use of temperature and heat transfer coefficient boundary conditions on the model. Research have shown that the furnace process heat transfer coefficient in the lower stack of the blast furnace is approximately 127 J/sm^2 °F [7]. This is coupled with a process temperature of 2000°F to account for the heat transferred to the refractory from the furnace process. Heat is removed from the system by forced convection into the cooling palates or stave pipes and by free convection and radiation off the shell.

The heat transfer coefficient for the inside surface of the cooling plate can be approximated by use of the widely accepted correlations for forced convection in cooling passages [8]. However, the heat transfer coefficient for a stave-cooling pipe must account for the inherent separation layer between the cooling pipe and the stave as a result of the casting process. This operation furnace condition so established was then used as the boundary conditions for the model

MATERIAL PROPERTIES

Upon defining the model geometry and boundary conditions, the appropriate material properties are input to the model. Typical values of the ultimate strength and the temperature limits for various furnace refractory materials are given in table 1 below (4).

Table 1: Properties of lining materials [8]

Types of Refractory	Ultimate compression strength* kN/cm^2 (kgf/cm^2)	Temperature of softening at 20 N/cm^2. °C	Refractoriness
Silica	2.45 – 2.94 (245 – 294)	1630	1730
Fireclay	0.98 – 6.88 (98 - 688)	1350	1730
Magnesite	2.94 – 4.90 (294 - 490)	1500	2000
Chrome Magnesite	2 – 5 (200 - 500)	1520	2000
Periclese - Spinelide	4 – 8 (400 - 800)	1530	2000

At room temperature

Material Interface Considerations

The major simplifying assumption in the analysis of furnace refractory linings is to assume perfect contact between material surface interfaces especially when the materials have a very smooth surface. In order to qualify this assumption, the effect of thermal contact resistance would have to be shown to be insignificant relative to the thermal resistance of the refractory mass.

The general effect of thermal contact resistance for two surfaces can be seen by comparing figures 3 and 4 below. The idealized surface has perfect contact between the two materials and a continuous temperature profile, thus the temperature at the interface is identical for both materials. This is the case even though the two contacting materials have different conductivities resulting in a discontinuity in material properties at the contact surface. The real surface is characterized by imperfect contact at the material interface resulting in a finite separation at the contact surface. This results in discontinuity in the temperature profile at the material interface. Heat transfer across the gap can take place in the form of radiation, convection, and conduction across the interstitial fluid and by material to material conduction at the points of intimate contact. The effects of the finite gaps at the interface of the real materials are usually accounted for in the form of a contact conductance heat transfer coefficient (the contact resistance is the reciprocal of this value and the terms will be used interchangeably throughout). The corresponding heat flux for the real system, 'Q', is reduced by an amount proportional to the magnitude of thermal contact resistance at the interface. Some of the parameters influencing this contact resistance are;

(a) The thermal conductivities of the two materials
(b) The interface pressure
(c) Surface roughness
(d) Material modulus of elasticity
(e) Mean contact temperature level
(f) Interstitial fluid properties

The only item, which the refractory designer can practically address, is the surface roughness which can be improved upon by machining the respective contact surfaces to enhance the amount of true contact area at the material interface, thus reducing the magnitude of the thermal contact resistance (increase the magnitude of the thermal contact conductance).

Various empirical and semi-empirical correlations exist for calculating the magnitude of thermal contact resistance taking into account the above parameters [9]. Recognizing the wide range of operating conditions that refractory in a furnace must endure, the most practical approach to evaluating the effect of thermal contact resistance is to identify an order of magnitude value and include this in the finite element model. The results of this model will give the designer a qualitative approach of how this contact resistance affects refractory cooling. If the effects of thermal contact resistance for this range of value prove to be significant in a refractory cooling model then a more precise value must be determined, which is subject of future research work.

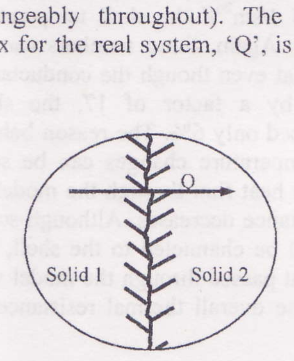

PERFECT CONTACT

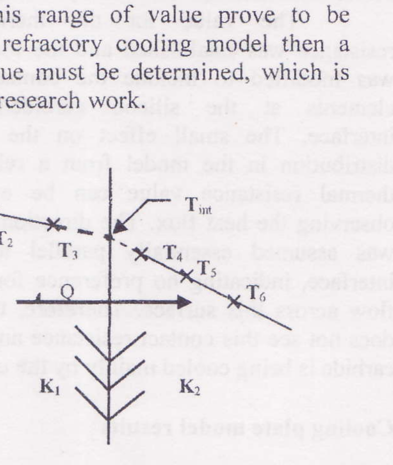

Figure 3: Linear Heat Flow across Ideal Interface

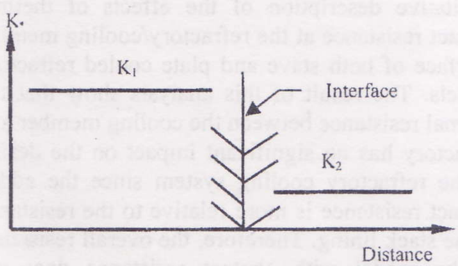

DISCONTINUITY OF K

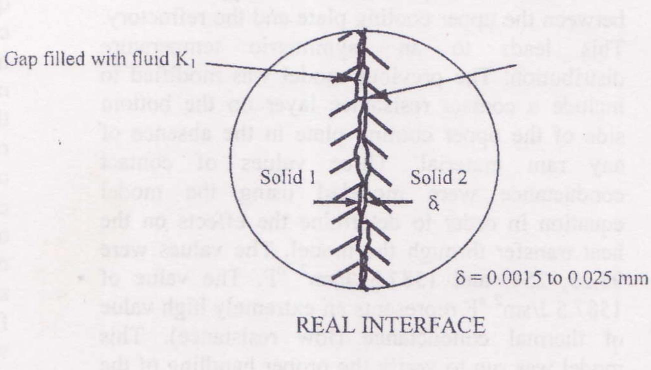

REAL INTERFACE

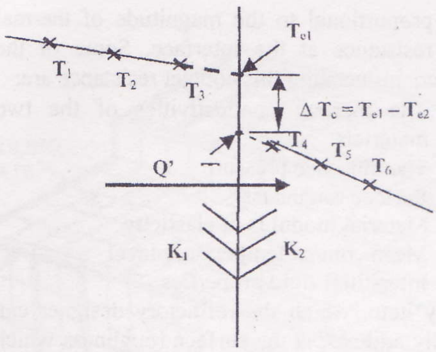

Figure 4: Linear Heat Flow across a Real Interface

RESULTS

Stave model results

A simple but effective approach in determining the effect of thermal contact resistance is to isolate the region of refractory/cooling member, recognizing that contact resistance in this area will be likely to impede heat transfer more than any other region of the lining.

The effective heat transfer from the material (silicon carbide) to the stave body and cooling pipes is essential to the performance of the silicon carbide. When the appropriate boundary conditions are applied to this model, the resulting thermal profile shows the temperature variation across the materials.

The value for the thermal contact resistance was established and the thermal model was modified to include the contact resistance elements at the silicon carbide/stave ledge interface. The small effect on the temperature distribution in the model from a relatively high thermal resistance value can be explained by observing the heat flux. The direction of heat flux was assumed essentially parallel to the brick interface, indicating no preference for the heat to flow across this surface. Therefore, the heat flux does not see this contact resistance and the silicon carbide is being cooled mainly by the upper stave.

Cooling plate model results

The refractory arrangement for the cooling plate is modeled in such a way that there is a ram between the lower plate and refractory, but no ram between the upper cooling plate and the refractory. This leads to an asymmetric temperature distribution. The previous model was modified to include a contact resistance layer on the bottom side of the upper cooling plate in the absence of any ram material. Three values of contact conductance were modeled using the model equation in order to determine the effects on the heat transfer through the model. The values were 95.25, 254, and 1587.5 J/sm^2 °F. The value of 1587.5 J/sm^2 °F represents an extremely high value of thermal conductance (low resistance). This model was run to verify the proper handling of the thermal contact resistance by the finite element model. Also, the results in table 2 show the total heat flux through the model.

Table 2: Results of Thermal analysis

Contact Conductance (J/sm^2 °F)	Maximum shell Temperature (oF)	Heat Fluxes through the shell (J/sm^2 °F)
95	245	355
160	242	352
225	241	346
320	240	341
475	239	337
795	237	333
925.5	237	331
1270	236	328
1587.5	235	326

The table shows the effect that varying values of contact conductance has on the heat transfer through the model. As the value of contact conductance is decreased, the amount of heat transfer through the cooling plate is decreased. There is also a rise in amount of heat transferred through the shell and corresponding rise in shell temperature. It should be noted that the relative rise in shell temperature is small compared to the decrease in contact conductance. When the contact conductance is decreased from 1587.5 to 225 J/sm^{2o}F the resulting shell temperature only increases from 235°F to 243°F. In other words, the value of contact conductance decreased by a factor of 6 while the shell temperature increased only 3%. Similarly, when the contact conductance is decreased to 95.25 J/sm^{2o}F the shell temperature increases to 249°F. Again, these numbers can be reduced to show that even though the conductance decrease roughly by a factor of 17, the shell temperature increased only 6%. The reason behind the small shell temperature changes can be seen examining the total heat flux through the model as the contact conductance decreases. Although some additional heat will be channeled to the shell, the total amount of heat passed through the model will decrease due to the overall thermal resistance of the model.

CONCLUSIONS

Finite element modelling was used to obtain a qualitative description of the effects of thermal contact resistance at the refractory/cooling member interface of both stave and plate cooled refractory models. The result of this analysis show that the thermal resistance between the cooling member and refractory has no significant impact on the design of the refractory cooling system since the added contact resistance is more relative to the resistance of the stack lining. Therefore, the overall resistance of the model with contact resistance does not significantly increase. This explains why the heat flux through the model does not vary appreciably with different values of contact resistance hence the effect of machining to improve the surface roughness and hence creating a more intimate contact between the refractoties and cooling members will not produce any appreciable gain.

REFERENCES

V. Krivandin. B. Markov, 1980, Metallurgical Furnaces, Mir Publishers.

Incropera, F. P., Dewitt, D. P. (1981), "Fundamentals of Heat Transfer", John Wiley & Sons.

E. I. Kazantser, 1977, Industrial Furnaces, Mir Publishers, Moscow.

Attilio, M. Colangelo, (1999), "Finite Element Thermal Analysis applied to Blast Furnace", ASTI, Inc; Buffalo, New York.

Yildiz Bayazitoglu, M. Necati √zi]]ik, 1976, Elements of Heat transfer, McGraw – Hill Book Company, United states.

Grundtish, D. P. (1990), "Application of finite element Analysis to Blast Furnace Design" AIME Conference, Detroit, Michigan

Helenbrook, R. C.; Cox I. J.; Grundtish, D. P.; "Utilization of Operational Data to Predict Blast Furnace Refactory/Cooling System Performance", 1983 AISE Convection.

Sparrow, E. M., Cess R. D., 1967, Radiation Heat Transfer, Wadsworth Publishing Company, Inc., United states of America.

Yovanovich, M. M.; "Thermal Contact Resistance: Theory and Application" ASME Heart Transfer Conference, Niagara Falls 1984.

General Electric Company- Corporate Research and Development, "Heat Transfer Data Book", Schenectady, New York; July 1977.